

This is an Open Access document downloaded from ORCA, Cardiff University's institutional repository:<https://orca.cardiff.ac.uk/id/eprint/176954/>

This is the author's version of a work that was submitted to / accepted for publication.

Citation for final published version:

Akash, R., Sarathi, R. and Haddad, Manu 2025. Hybrid Swin Transformer approach for hydrophobicity monitoring of outdoor polymeric insulators in transmission lines. *IEEE Transactions on Dielectrics and Electrical Insulation* 10.1109/tdei.2025.3548969

Publishers page: <https://doi.org/10.1109/tdei.2025.3548969>

Please note:

Changes made as a result of publishing processes such as copy-editing, formatting and page numbers may not be reflected in this version. For the definitive version of this publication, please refer to the published source. You are advised to consult the publisher's version if you wish to cite this paper.

This version is being made available in accordance with publisher policies. See <http://orca.cf.ac.uk/policies.html> for usage policies. Copyright and moral rights for publications made available in ORCA are retained by the copyright holders.



Hybrid Swin Transformer Approach for Hydrophobicity Monitoring of Outdoor Polymeric Insulators in Transmission Lines

R Akash, Graduate *Member, IEEE* R. Sarathi, *Senior Member, IEEE*, and Manu Haddad, *Member, IEEE Member*

Abstract— Hydrophobicity is one of the vital properties of outdoor polymeric insulators which prevents the water accumulation on the insulator's surface. Due to extreme environmental conditions, polymeric insulators tend to lose its hydrophobicity property. Accurate hydrophobicity classification is essential to know the healthiness of the insulators in operation in the power system network. In this study, a Hybrid Swin Transformer (HSW) is designed to enhance the hydrophobicity classification accuracy. Traditional image classification methods struggle with variation in droplet shapes, sizes and surface patterns which can complicate the classification process but proposed model integrates hybrid shifted windows with advanced vision transformer techniques to capture both short-range and long-range dependencies in images, providing a more robust understanding of complex visual patterns associated with different hydrophobicity levels. This Hybrid approach has been evaluated with laboratory generated dataset (according to IEC Standard 62073) and an online available dataset. Extensive experimental and analytical results demonstrate that the proposed hybrid model outperforms existing state-of-the-art techniques. Additionally, an android application for image classification was developed with a simple graphical user interface (GUI) to enhance the insulator's maintenance.

Index Terms— Hybrid Swin Transformer, hydrophobicity, image classification, polymeric insulators and visual patterns

I. INTRODUCTION

OVER the past few decades, silicone rubber based polymeric insulators have gained significant traction in electrical power system networks [1]. Polymeric insulators have high mechanical strength, lightweight in nature, outstanding dielectric properties and expectational pollution performance, which enabled one to use as insulation structure in both transmission and distribution lines [2]. These insulators when they are installed in harsh environmental condition, they tend to degrade over a period of time which eventually affects the performance of the insulator [3]. Hydrophobicity is a critical property of the polymeric insulators, which can be a potential indicator of the degradation level [4]. Therefore, it is essential to have a periodical inspection of the hydrophobicity of

insulators in operation, for ensuring the proper and reliable operation of the power system.

The International Electrotechnical Commission (IEC) 62073 guidelines provide three major techniques to measure the hydrophobicity of the insulator [5]. The first method is the Contact Angle (CA) measurement, which is a popularly known method where the angle formed by the water droplet on the surface of the material is measured. CA gives accurate results about the hydrophobicity but demands sophisticated laboratory equipment. Second method is surface tension approach which quantifies the hydrophobicity based on the surface tension but this method also requires specialized equipment making it much difficult for practical use in the field. The third method is spray method which is widely used in the field due to its simplicity. In this method deionized water is sprayed on the surface of the insulator at an angle and photographs are taken [6]. The hydrophobicity of the insulator is assessed by the operator's judgement. Nevertheless, a significant drawback of this approach is that the evaluation relies on human knowledge, and the dependability of human judgment might result in variations in hydrophobicity classification.

To overcome this issue, the world over researchers have explored various techniques like digital image processing [7], machine learning [8] [9] and pattern recognition [10] to improve the quality of the assessment. Berg et al. [11] conducted a study on numerical image analysis method to assess the hydrophobicity of polymeric insulator surfaces by examining water drop patterns. Average of Normalized Entropies (ANE) is introduced in this study to correlate with the traditional hydrophobicity classifications and is robust to variations in photographic setup and surface inclination. In a study conducted by Khaled et al. [12] evaluated different feature extraction techniques to classify insulator hydrophobicity classes. It is reported that adopting artificial neural network (ANN) consisting of three layers and utilizing certain feature sets showed improved classification rates. The hydrophobic properties of polymeric outdoor insulator were observed by Thomazini et al [13] by employing three digital image processing techniques: fractal dimension, Haralick features

This work was supported by the Central Power Research Institute (CPRI), Bangalore, India, under Grant CPRI/R&D/TC/GDEC/2023.

R Akash and R. Sarathi are with the Department of Electrical Engineering, Indian Institute of Technology Madras, Chennai 600036, India (e-mail: ee22d034@smail.iitm.ac.in ; sarathi@ee.iitm.ac.in).

Manu Haddad is with the School of Engineering, Cardiff University, Cardiff, U.K. (haddad@cardiff.ac.uk)

(homogeneity and entropy), and a wide range of filters. The Haralick's homogeneity feature combined with the White Top-Hat filter showed better performance. Huang et al [14] utilized Binary Large Object (BLO) analysis and morphological processing techniques to accurately segment water droplets. It is reported to achieve an identification rate of 91% on a set of 140 test samples. Nevertheless, it encounters obstacles as a result of environmental conditions and the possibility of contamination. Sun et al [15] employed wavelet denoising and Retinex enhancements to insulator images for hydrophobicity classification. In this study they utilized two-dimensional adaptive Otsu's method to separate water droplets from the surface of the insulator using Probabilistic Neural Network. Conventional image processing and machine learning techniques have difficulties in effectively capturing complex droplet patterns on polymer insulators because they heavily rely on manually extracted features. This might affect the efficiency of classification tasks. Deep learning-based approaches, especially Convolutional Neural Network (CNN) have employed by researchers to overcome this issue of feature extractions because CNNs can automatically extract features of an image like texture, size, shape and patterns. Soumya et al [16] adopted digital image processing techniques, a deep-learning framework featuring convolutional neural networks, transfer learning, and several CNN designs. It is reported that training the CNN models for hydrophobicity classification from the scratch is time consuming. Despite its high accuracy CNNs suffers with drawbacks like computational complexity, overfitting when trained with a smaller number of data, lagging long term dependencies and difficult interpretations. Recently, researches have proven that Vision Transformers (ViT) has the potential to overcome the aforementioned drawbacks. ViT takes fixed-size patches as input, which are then flattened and transformed into vectors. These vectors are then sent into the Transformer layer and transformer layer performs self / cross-attention operations, allowing it to capture long-range dependencies. Although ViT has several benefits, it falls short in identifying complex pictures compared to CNN-based classifiers because it struggles to capture detailed local context as ViTs uses global self-attention mechanisms and lacks inductive bias. In order to get competitive outcomes, ViT requires prior training on large datasets such as JFT300M. To overcome the limitations of the conventional ViTs, a novel approach is followed in Swin Transformer utilizing local self-attention rather than using global self-attention. Swin transformers can capture long – range dependencies as computes attention, non-overlapping windows, enabling better interaction between these windows. Additionally, Swin transformer uses hierarchical architecture similar to that of a CNN.

Having known the above-mentioned concerns, this study a Hybrid Swin Transformer (HSW) approach is developed for efficient classification of hydrophilicity in outdoor polymeric insulators. The developed model is trained and tested with laboratory generated dataset as well as publicly available dataset. This study includes CLAHE (Contrast Limited Adaptive Histogram Enhancement) for preprocessing of the

images and the performance of the proposed HSW models is compared with standard Swin transformer and other state of the art models. Additionally, the developed image classification model is deployed in a android application to enhance the real time decision strategy of the operator in the field.

II. EXPERIMENT AND METHODOLOGY

A. Datasets Description

In this study, two different datasets were utilized. One is laboratory generated dataset which will be referred as Dataset – I and an online available dataset which will be referred as Dataset – II [17]. The Dataset – I involve 11kV outdoor polymeric insulators in different colours like red, grey and white. These insulator sheds are cleansed with ethanol to get rid of dirt and the samples were dried before spraying. The duration of each spraying session was consistently maintained for at least 10 seconds to guarantee a good interaction between the solution and the surface of the insulator. A total of 300 photos were captured for each hydrophobic condition, with 100 photographs obtained for every colour of the insulator. Dataset-I consisted of 2,100 photos, providing an extensive range of samples. This study employed the spray method outlined by the Swedish Transmission Research Institute (STRI) and adhered to the guidelines specified in IEC TS 62073. The aim was to systematically vary the volume percentage of isopropyl alcohol in distilled water from 0% to 100% in order to generate diverse hydrophobic conditions.

The Dataset II, developed by Kokalis et al.[17], is a well-known database consisting of 4,500 images categorized into seven distinct hydrophobicity classes. These images were collected from ten suspension-type and ten post-type silicone rubber insulators, each rated for 24 kV. For the image acquisition process, a Nikon D3200 camera equipped with an AF-S DX NIKKOR 18–55-mm f/3.5–5.6G VR II lens was utilized. From this comprehensive dataset, 3,500 images were selected for classification, ensuring that each hydrophobicity class was represented by 500 images. Fig 1 displays random sample images belonging to Dataset – II.

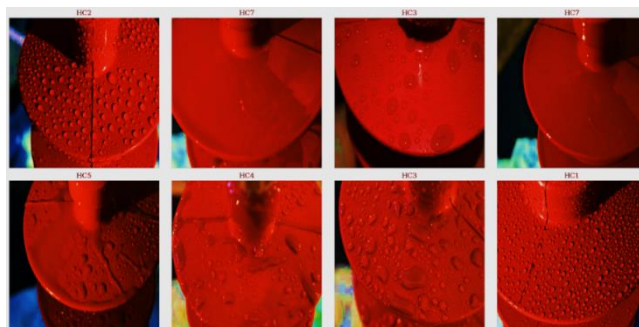


Fig. 1. Insulator Hydrophobicity Images of Different classes.

B. Methodology

The Swin Transformer employs a hierarchical architecture to effectively capture image details at multiple scales, enhancing both training efficiency and feature detection across various levels of scale. However, this structure limits the model's ability to capture global context information, especially for insulator

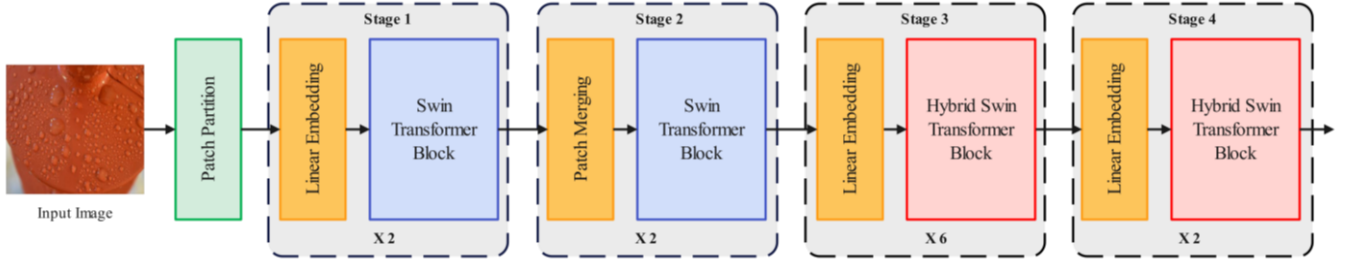


Fig. 2. Architecture of the proposed Hybrid Swin Transformer.

hydrophobicity images. To overcome these issues in this study a Hybrid Swin Transformer approach is proposed. The Hybrid Swin Transformer incorporates hybrid shifted windows by combining long rectangular shaped windows along with the traditional shifted windows. The proposed architecture enables the model to capture both local and global distributions in images. The long rectangular windows enable the model to capture extensive regions of interest, while traditional shifted windows focus on localized features

C. Architecture

Fig 2 illustrates the architecture of the proposed Hybrid Swin transformer model for classifying hydrophobicity of the polymeric insulator. The architecture begins with preprocessing the input image of size $H \times W \times 3$. The patch partition module is used to extract non-overlapping patches of size 4×4 from the input image. This results in $(H/4) \times (W/4)$ patch tokens. Each patch, which is formed by combining raw pixel values, has a feature dimension of 48, calculated as $4 \times 4 \times 3$. In this approach, every image patch is first treated as an individual "token." Afterward, a linear embedding layer is employed to modify the dimensionality of these tokens to a predetermined value. The network is organized into four steps in order to construct a hierarchical representation of the data. Each stage comprising a series of transformer blocks. In this study, the Swin-T architecture serves as the base model, with the number of blocks configured as 2, 2, 6, and 2 for Stages 1 through 4, respectively. The initial two stages utilize standard Swin Transformer blocks, whereas the final two stages are constructed using Hybrid Swin Transformer blocks. It is noteworthy to mention that the feature dimensions remain constant within each stage. The patch merging which is applied between two stages operates in a manner similar to a pooling layer by reducing the feature dimensions. Patch merging is a technique that simplifies dimensionality reduction by merging neighbouring 2×2 tokens into a single feature. The resulting feature has a dimensionality four times larger than the original token dimension, which is represented as $4C$. Afterwards, a linear layer is used to decrease the dimension of the merged token to $2C$. The process of merging and lowering dimensions in this approach results in the formation of a hierarchical structure that is similar to the one employed in Convolutional Neural Networks (CNNs).

D. Swin Transformer

Fig 3 depicts the structure of a typical Swin transformer module. Liu et al [18]. implemented self-attention within a limited window to enhance the computational efficiency of the

Swin transformer. While the window-based self-attention method is efficient, it is limited in its ability to capture global dependencies. This occurs due to the processing of information within fixed-sized windows, which hinders the development of links across many windows. In order to overcome this constraint, the Swin Transformer incorporates shifted window self-attention alongside the existing window-based self-attention. This technique allows the model to capture relationships across multiple windows by utilizing self-attention across shifted windows. A typical Swin Transformer block comprises two types of multi-head self-attention (MSA) layers: the window-based MSA and the shifting window-based MSA. Each of these layers is followed by a two-layer Multilayer Perceptron (MLP).

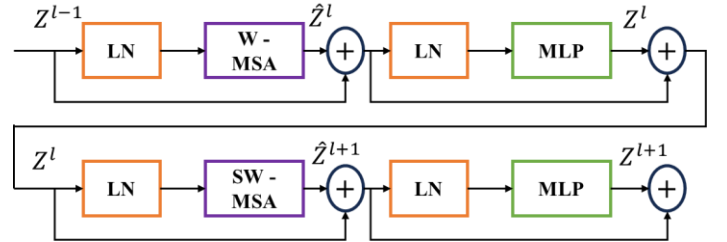


Fig. 3. The structure of typical Swin Transformer module

Additionally, both the MSA and MLP layers are preceded by a Layer Norm (LN) layer. The purpose of this LN layer is to normalize the inputs in order to stabilize and improve the training process. The standard Swin Transformer blocks are computed as:

$$\hat{Z}^l = W - MSA(LN(Z^{l-1})) + Z^{l-1} \quad (1)$$

$$Z^l = MLP(LN(\hat{Z}^l)) + \hat{Z}^l \quad (2)$$

$$\hat{Z}^{l+1} = SW - MSA(LN(Z^l)) + Z^l \quad (3)$$

$$Z^{l+1} = MLP(LN(\hat{Z}^{l+1})) + \hat{Z}^{l+1} \quad (4)$$

From the above equations it is understood that Z^l represents the output features from the Multilayer Perceptron (MLP) in block l , while \hat{Z}^l represents the estimated output features. The term " l " represents the output features obtained by the MSA in block " l ". The abbreviation W-MSA stands for window-based multi-head self-attention module, while SW-MSA represents the shifted window-based multi-head self-attention module. Fig 4 illustrates the division of the window in the basic Swin Transformer blocks.

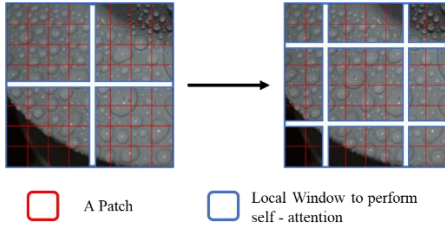


Fig. 4. Window partition in typical Swin Transformer

E. Hybrid Swin Transformer

Fig 5 illustrates the structure of the hybrid Swin Transformer unit, which consists of two stages: the typical window-based multi-head self-attention layer and the hybrid shifting windows-based multi-head self-attention (HSW-MSA) layer.

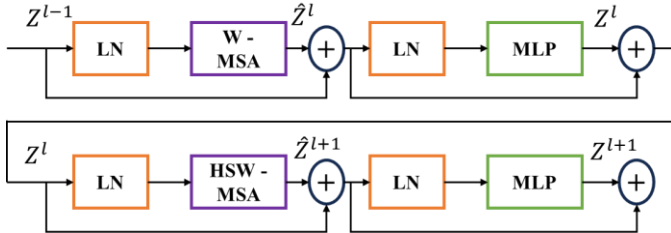


Fig. 5. The structure of Hybrid Swin Transformer module

Fig 6 depicts the presence of elongated rectangular windows in the Swin Transformer's hybrid shifted windows. These windows can shift both horizontally and vertically, in addition to the regular shifted windows. The multi-head self-attention mechanisms in the HSW-MSA layer are divided into three separate groups to facilitate specialized processing. In this arrangement, exactly half of the total multi-heads are allocated to the first group, which carries out standard self-attention using the shifted window technique.

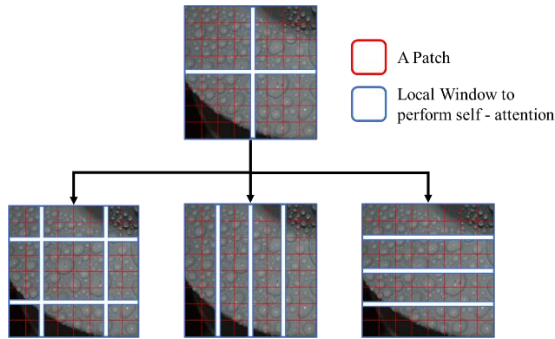


Fig. 6. Window partition in Hybrid Swin Transformer

The second group, including 50% of the remaining multi-heads, is dedicated to self-attention utilizing horizontal strip windows. Lastly, the final quarter of the multi-heads is allocated for performing self-attention using vertical strip windows. The computation for the hybrid shifted window transformer unit can be expressed as:

$$\hat{Z}^l = W - MSA(LN(Z^{l-1})) + Z^{l-1} \quad (5)$$

$$Z^l = MLP(LN(\hat{Z}^l)) + \hat{Z}^l \quad (6)$$

$$\hat{Z}^{l+1} = HSW - MSA(LN(Z^l)) + Z^l \quad (7)$$

$$Z^{l+1} = MLP(LN(\hat{Z}^{l+1})) + \hat{Z}^{l+1}. \quad (8)$$

III. RESULTS AND DISCUSSION

A. Data Preprocessing - CLAHE

In this study, Contrast Limited Adaptive Histogram Equalization (CLAHE) is employed for preprocessing to enhance the quality of the insulator hydrophobicity images before feeding to classification models [19]. CLAHE is particularly effective for improving image contrast in a manner that is sensitive to local variations. CLAHE partitions a picture into smaller sections and performs histogram equalization on each section individually. This process improves the contrast in areas of the image that have different colours and different lighting conditions [20]. Enhancing contrast facilitates clearer feature extraction and improves the performance of classification models. This allows the model to more effectively capture and understand significant features, leading to improved analysis of hydrophobicity. Fig 7 displays the images enhanced by CLAHE for all three colours of the insulator: red, grey, and white.

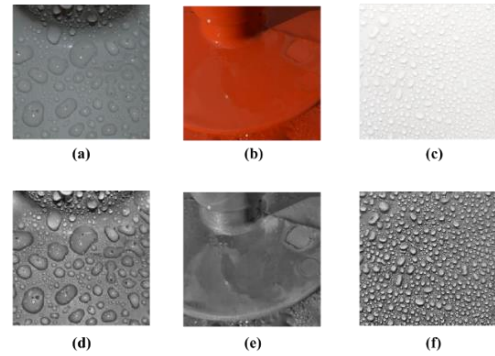


Fig 7. (a-c) Original images (d-f) CLAHE enhanced images

B. Comparative Studies

This study compared advanced machine learning classifiers and deep learning networks, specifically VGG-16, VGG-19, DenseNet, Swin transformer, and Vision Transformer (ViT) for hydrophobicity classification. The Visual Geometry Group (VGG) created the VGG-16 model specifically for large-scale visual recognition tasks [21]. This model features a total of 16 layers and primarily relies on 3×3 convolutional layers as its backbone. Each of these convolutional layers uses the rectified linear unit (ReLU) activation function, and the architecture incorporates 2×2 max pooling layers to help reduce the dimensionality of the data. To produce final predictions, VGG-16 also includes three fully connected layers. On the other hand, the VGG-19 model builds upon this architecture by adding three additional convolutional layers, which enhances its ability to extract features from images. In contrast, DenseNet takes a different approach. Instead of just passing information to the next layer, each layer in DenseNet connects to all subsequent layers. This means that every layer can reuse feature maps from all previous layers. Furthermore, the compact design of DenseNet keeps the number of hyperparameters in check. In this study, the hyper-parameters for the Swin and hybrid Swin

model architectures are as follows: Swin Transformers: The initial stage contains hidden layers with 96 channels. The architecture comprises layer configurations of 2, 2, 6, and 2 across successive stages. Additionally, the number of attention heads in each stage is set to 3, 6, 12, and 24, respectively. HSW Transformers: This model also starts with 96 channels in the hidden layers of the first stage. The architecture includes 2, 2, 6, and 2 layers across its stages. The number of attention heads in each stage is 6, 12, 24, and 48, respectively. The neural networks were trained and evaluated for 200 epochs, with the first 25 epochs specifically dedicated to warm-up. The models were run 10 times each, and the mean value was calculated and compared against different models.

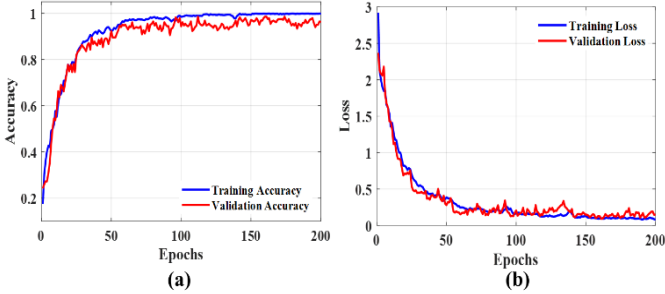


Fig 8 (a) Accuracy and (b) Loss variation with variation in epochs

The Python implementation utilized popular libraries including PyTorch, Keras, TensorFlow, Scikit-learn, and NumPy. The model was deployed on an Nvidia RTX 4060 GPU that supports CUDA. The computations were executed on an Intel i9 13th generation laptop with 16GB of RAM. Accuracy and F1 score are the two major performance metrics chosen to evaluate and compare these models and it can be computed as follows:

$$Accuracy = \frac{TP + TN}{TP + TN + FP + FN} \quad (9)$$

$$F1\ Score = \frac{2 \cdot TP}{2 \cdot TP + FP + FN} \quad (10)$$

TP, TN, FP, and FN represent the number of true positives, true negatives, false positives, and false negatives, respectively. Fig 8 shows the accuracy and loss response with respect to increase in number of epochs during training and validation. Table I provides the performance comparison for various state of the art model with two different datasets.

TABLE I

PERFORMANCE COMPARISON AGAINST VARIOUS MODELS

Model	Dataset I		Dataset II	
	Accuracy	F1 - Score	Accuracy	F1 - Score
VGG16	94.51%	0.89	94.51%	0.89
VGG19	95.24%	0.87	95.24%	0.87
DenseNet	95.71%	0.92	95.71%	0.92
ViT	92.28%	0.91	92.28%	0.91
Swin	95.82%	0.89	95.82%	0.89
Proposed	98.47%	0.98	98.47%	0.98

The results shows that the proposed hybrid Swin Transformer surpasses conventional models in terms of accuracy and F1 score, showcasing its effectiveness in tackling class imbalances and providing persistent predicting performance.

For further analysis, in this study t-SNE plot is utilized. The t-SNE plot is a tool that visually displays the distribution and separation of feature embeddings from the proposed hybrid Swin transformer model. Fig 9 (a) shows the t-SNE plot obtained from the proposed model for the Dataset – II. Additionally, to highlight the model’s performance the decision boundaries from an logistic classifier are overlaid on the plot in Fig 9 (b).

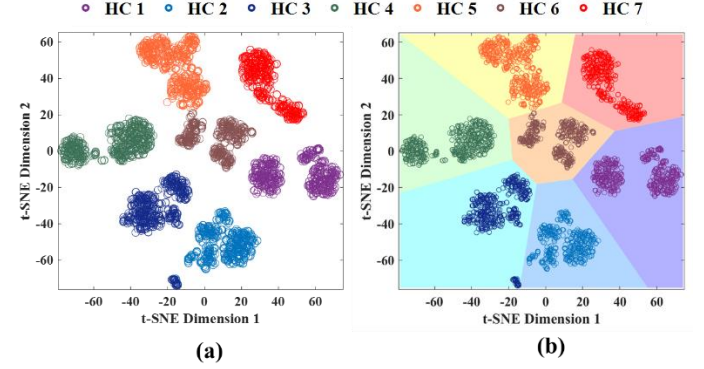


Fig. 9. T-SNE plot for low-dimensional visualization: (a) trained network; and (b) decision boundary for Logistic classifier.

To further understand the limitation of the existing models and to identify the most problematic class, the proportion of classification errors of each class across various models are compared for the Dataset - II.

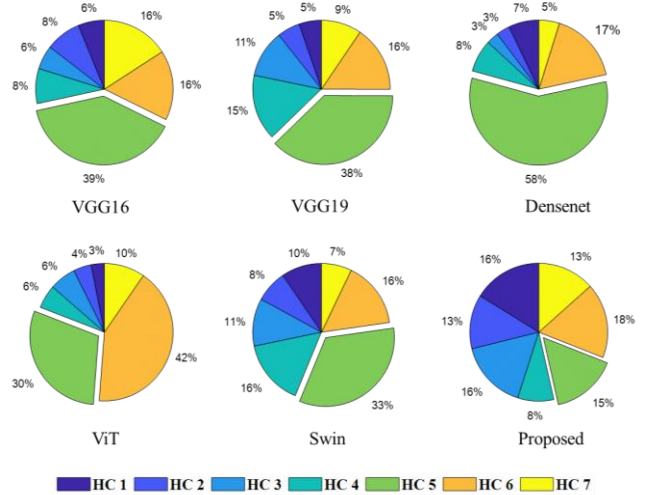


Fig 10 Proportion of classification errors

From the Fig.10 it is clear that most of the classification error occurs with HC 5 class. From the sample images in Fig 10 it can be seen that during the class HC 5, the insulator images start to exhibit the hydrophilic behaviour. This transition can make it challenging for models to accurately categorize insulators. The experimental findings validate the claim that models that

TABLE II
PERFORMANCE COMPARISON AGAINST EXISTING LITERATURE

Author	Model	Image Enhancement	Indoor / Outdoor Implementation	Android Application	Accuracy (%)
Jayabal et al [23]	ANFIS	-	-	-	93.30
Sun et al [15]	Improved Probabilistic Neural Network	-	-	-	94.80
Yang et al [24]	Back Propagation	-	-	-	98.10
Jarrar et al [12]	ANN	-	-	-	96.5
Paul et al [25]	Res-Morph-NN	✓	-	-	98.29
Kokalis et al [17]	GoogLeNet	-	-	-	97.68
Modak et al [16]	AlexNet	-	-	-	96.4
Yu et al [26]	ShuffleNet 0.5×	-	✓	-	97.09
This paper	Hybrid Swin Transformer	✓	✓	✓	99.2

depend on local features encounter challenges with effectively detecting appropriate regions within images. Long-range dependencies must be incorporated into the Swin Transformer model to address this issue. Furthermore, it is evident from Fig 10 that the proposed approach has enhanced the classification performance.

Additionally, the performance of the proposed Hybrid Swin Transformer is compared against various other methods available in the literature (Table II). The results indicate that the proposed method performs similarly to, or in some cases, exceeds the performance of existing approaches. Table provides a comprehensive comparison and highlights the proposed method against existing literature. It is noteworthy to mention that this comparison is based on Dataset-II to ensure fairness. From the tabulated data it is clear that the proposed method, with 99.2% accuracy, supports both indoor and outdoor implementations and includes an Android application.

C. Grad-CAM Visualization

The main advantage of transformer-based models is that the trained model can interpret its own classification results. Heatmaps of activations are the most informative way for showing the representations learned by vision transformers. In this current study, Gradient Weighted class Activation Mapping (Grad-CAM), a well-established method is utilized for plotting visual explanation of the classification results given by both Swin Transformers as well as hybrid Swin transformer models [22]. Grad-CAM highlights the importance of individual locations in the input image with respect to the class being considered. Figs 11b and 11c illustrate the application of the Grad-CAM method on the test images employed in this investigation. The Swin Transformer selectively focuses its attention on specific Regions of Interest (ROIs) within the given statistics, which are visually emphasized using different shades of yellow.

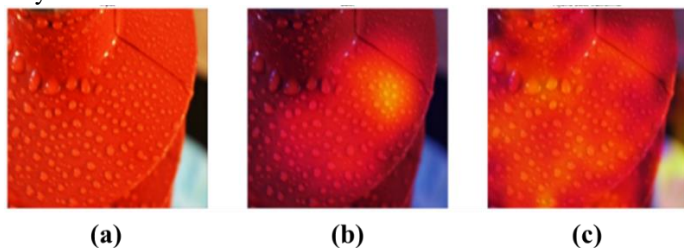


Fig.11 Visual interpretation using Grad-CAM (a) Input Image (b) Swin Transformer response (c) Hybrid Swin Transformer response

From the Fig 11 (c) it can be observed that HSW Grad-CAM displays a more focused and relevant activation map, with highlighted areas closely corresponding to image features, while Swin transformer's visual response appears to be scattered and less informative, making it difficult to identify specific regions.

D. Ablation Studies

This section assesses the effectiveness of the proposed method by substituting the SW-MSA with HSW-MSA at various stages. This ablation study is performed an experiment utilizing both Dataset – I and Dataset – II to examine two scenarios: the replacement of blocks solely in stage 4 vs the replacement of blocks in both stages 3 and 4.

TABLE III
EFFECTS OF REPLACING HYBRID SWIN TRANSFORMER MODULE

Parameters	Only in Stage 4		Stage 3 & 4	
	A	B	A	B
Accuracy	93.24	94.89	98.47	99.22
F1 Score	0.84	0.83	0.97	0.98

*A and B represents Dataset-I and Dataset-II

The results tabulated in Table III demonstrates that substituting blocks in the third and fourth phases produces superior outcomes compared to solely replacing the final stage. This supports the proposed analysis, indicating that incorporating elongated rectangular shifted windows within Hybrid Swin Transformer blocks improves the model's capacity to capture long-range dependencies.

E. Android Application

In this study, the proposed model is incorporated through an Android application for hydrophobicity classification. The application was built using Android Studio and incorporates TensorFlow Lite to power the trained model's capabilities directly on mobile devices. The app is developed with a simple graphical user interface (GUI) which facilitates straightforward interaction for the operator. The app is developed in such a way that the operator has to just take / upload the photo of the sprayed insulator sample and app gives the real time classification results along with the probability score. This probability score enhances the operator by offering a measure of confidence in the classification results. The best accuracy

was achieved when the photographs were taken from a distance of 25-30 cm away from the sample. The app has been tested in both indoor and outdoor conditions as demonstrated in Fig 12.

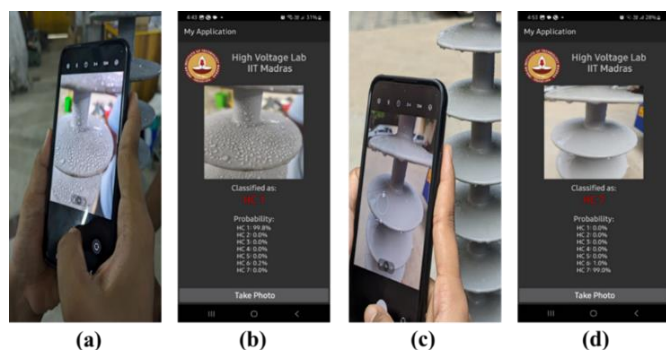


Fig 12. (a) Photograph captured in indoor (b) and (d) classification results with probability score (c) and (d) photograph captured in outdoor

IV. CONCLUSION

In this study a novel hybrid Swin transformer approach is proposed for hydrophobicity classification of the outdoor polymeric insulators. The hybrid model effectively combines the ability of the Swin transformer which captures the multi-scale features while overcoming its limitation in capturing the long-term dependencies. In this study two different datasets were utilized to evaluate the proposed hybrid approach. The insulator images were enhanced using contrast limited adaptive histogram equalization algorithm. The extensive experimental results carried out in this study demonstrates the hybrid approach's superior performance compared to existing state-of-the-art methods. The proposed methodology provides a non-destructive, cost effective and highly accurate means of classification results. Additionally, in this study an android application is developed and the image classification model is deployed. It integrates advanced image classification technology into a user-friendly mobile application, allowing real-time analysis and accurate assessment of insulator conditions, showcasing the practical benefits of machine learning.

REFERENCES

[1] L. Xidong, W. Shaowu, F. Ju, and G. Zhicheng, "Development of Composite Insulators in China," *IEEE Transactions on Dielectrics and Electrical Insulation*, vol. 6, no. 5, 1999.

[2] A. A. Salem et al., "Investigating and Modeling Ageing Effects on Polymeric Insulator Electrical Properties," *IEEE Access*, vol. 11, pp. 82132–82150, 2023, doi: 10.1109/ACCESS.2023.3298776.

[3] A. H. El-Hag, S. H. Jayaram, and E. A. Cherney, "Influence of Shed Parameters on the Aging Performance of Silicone Rubber Insulators in Salt-fog," 2003.

[4] R. A. Ghunem et al., "Development and Application of Superhydrophobic Outdoor Insulation: A Review," Aug. 01, 2022, Institute of Electrical and Electronics Engineers Inc. doi: 10.1109/TDEI.2022.3183671.

[5] Guidance on the measurement of hydrophobicity of insulator surfaces. International Electrotechnical Commission, 2016.

[6] G. Liu et al., "Monitoring of Composite Insulators in Transmission Lines: A Hydrophobicity Diagnostic Method Using Aerial Images and Residual Neural Networks," *IEEE Transactions on Power Delivery*, vol. 38, no. 4, pp. 2500–2509, Aug. 2023, doi: 10.1109/TPWRD.2023.3244840.

[7] Q. Wang, Z. Fan, Z. Luan, and R. Shi, "Insulator Abnormal Condition Detection from Small Data Samples," *Sensors*, vol. 23, no. 18, Sep. 2023, doi: 10.3390/s23187967.

[8] A. Ibrahim, A. Dalbah, A. Abualsaud, U. Tariq, and A. El-Hag, "Application of Machine Learning to Evaluate Insulator Surface Erosion," *IEEE Trans Instrum Meas*, vol. 69, no. 2, pp. 314–316, Feb. 2020, doi: 10.1109/TIM.2019.2956300.

[9] G. Liu et al., "Monitoring of Composite Insulators in Transmission Lines: A Hydrophobicity Diagnostic Method Using Aerial Images and Residual Neural Networks," *IEEE Transactions on Power Delivery*, vol. 38, no. 4, pp. 2500–2509, Aug. 2023, doi: 10.1109/TPWRD.2023.3244840.

[10] M. F. Palangar, S. Mohseni, A. Abu-Siada, and M. Mirzaie, "Online Condition Monitoring of Overhead Insulators Using Pattern Recognition Algorithm," *IEEE Trans Instrum Meas*, vol. 71, 2022, doi: 10.1109/TIM.2022.3209729.

[11] M. Berg, R. Thottappillil, and V. Scuka, "Hydrophobicity Estimation of HV Polymeric Insulating Materials Development of a Digital Image Processing Method," 2001.

[12] I. Jarrar, K. Assaleh, and A. H. El-Hag, "Using a pattern recognition-based technique to assess the hydrophobicity class of silicone rubber materials," *IEEE Transactions on Dielectrics and Electrical Insulation*, vol. 21, no. 6, pp. 2611–2618, 2014, doi: 10.1109/TDEI.2014.004523.

[13] D. Thomazini, M. V. Gelfuso, and R. A. C. Altafim, "Classification of polymers insulators hydrophobicity based on digital image processing," *Materials Research*, vol. 15, no. 3, pp. 365–371, May 2012, doi: 10.1590/S1516-14392012005000032.

[14] X. Huang, T. Nie, Y. Zhang, and X. Zhang, "Study on Hydrophobicity Detection of Composite Insulators of Transmission Lines by Image Analysis," *IEEE Access*, vol. 7, pp. 84516–84523, 2019, doi: 10.1109/ACCESS.2019.2922279.

[15] Q. Sun, F. Lin, W. Yan, F. Wang, S. Chen, and L. Zhong, "Estimation of the hydrophobicity of a composite insulator based on an improved probabilistic neural network," *Energies (Basel)*, vol. 11, no. 9, Sep. 2018, doi: 10.3390/en11092459.

[16] S. Chatterjee, S. S. Roy, K. Samanta, and S. Modak, "Sensing Wettability Condition of Insulation Surface Employing Convolutional Neural Network," *IEEE Sens Lett*, vol. 4, no. 7, Jul. 2020, doi: 10.1109/LENS.2020.3002991.

[17] C. C. A. Kokalis, T. Tasakos, V. T. Kontargyri, G. Siolas, and I. F. Gonos, "Hydrophobicity classification of composite insulators based on convolutional neural networks," *Eng Appl Artif Intell*, vol. 91, May 2020, doi: 10.1016/j.engappai.2020.103613.

[18] Z. Liu et al., "Swin Transformer: Hierarchical Vision Transformer using Shifted Windows," Mar. 2021, [Online]. Available: <http://arxiv.org/abs/2103.14030>

[19] Y. X. Tan, S. S. Fan, and Z. Y. Wang, "Global and Local Contrast Adaptive Enhancement Methods for Low-Quality Substation Equipment Infrared Thermal Images," *IEEE Trans Instrum Meas*, vol. 73, pp. 1–17, 2024, doi: 10.1109/TIM.2023.3342229.

[20] Z. Yuan et al., "CLAHE-Based Low-Light Image Enhancement for Robust Object Detection in Overhead Power Transmission System," *IEEE Transactions on Power Delivery*, vol. 38, no. 3, pp. 2240–2243, Jun. 2023, doi: 10.1109/TPWRD.2023.3269206.

[21] L. She, Y. Fan, M. Xu, J. Wang, J. Xue, and J. Ou, "Insulator Breakage Detection Utilizing a Convolutional Neural Network Ensemble Implemented With Small Sample Data Augmentation and Transfer Learning," *IEEE Transactions on Power Delivery*, vol. 37, no. 4, pp. 2787–2796, Aug. 2022, doi: 10.1109/TPWRD.2021.3116600.

[22] R. R. Selvaraju, M. Cogswell, A. Das, R. Vedantam, D. Parikh, and D. Batra, "Grad-CAM: Visual Explanations from Deep Networks via Gradient-Based Localization," *Int J Comput Vis*, vol. 128, no. 2, pp. 336–359, Feb. 2020, doi: 10.1007/s11263-019-01228-7.

[23] R. Jayabal, K. Vijayarekha, and S. Rakesh Kumar, "Design of ANFIS for hydrophobicity classification of polymeric insulators with two-stage feature reduction technique and its field deployment," *Energies (Basel)*, vol. 11, no. 12, Dec. 2018, doi: 10.3390/en1123391.

[24] L. Yang et al., "A Recognition Method of the Hydrophobicity Class of Composite Insulators Based on Features Optimization and Experimental Verification," *Energies (Basel)*, vol. 11, no. 4, Apr. 2018, doi: 10.3390/EN11040765.

[25] S. Chatterjee, S. S. Roy, A. Chatterjee, B. Ganguly, and S. Paul, "Recognition of Hydrophobicity Class of Polymeric Insulators

Employing Residual Morphological Neural Network and Granulometry-Based Image Analysis,” *IEEE Trans Instrum Meas*, vol. 71, 2022, doi: 10.1109/TIM.2022.3164156.

- [26] Z. Qiu, Z. Liu, C. Liao, D. Wang, and X. Yu, “Hydrophobicity Classification of Composite Insulators Based on Light-Weight Convolutional Neural Networks,” *IEEJ Transactions on Electrical and Electronic Engineering*, vol. 17, no. 12, pp. 1728–1737, Dec. 2022, doi: 10.1002/tee.23683.